

PCCP

Accepted Manuscript



This is an *Accepted Manuscript*, which has been through the Royal Society of Chemistry peer review process and has been accepted for publication.

Accepted Manuscripts are published online shortly after acceptance, before technical editing, formatting and proof reading. Using this free service, authors can make their results available to the community, in citable form, before we publish the edited article. We will replace this *Accepted Manuscript* with the edited and formatted *Advance Article* as soon as it is available.

You can find more information about *Accepted Manuscripts* in the [Information for Authors](#).

Please note that technical editing may introduce minor changes to the text and/or graphics, which may alter content. The journal's standard [Terms & Conditions](#) and the [Ethical guidelines](#) still apply. In no event shall the Royal Society of Chemistry be held responsible for any errors or omissions in this *Accepted Manuscript* or any consequences arising from the use of any information it contains.

Rate constants for collisional quenching of NO($A^2\Sigma^+$, $v=0$) by He, Ne, Ar, Kr, and Xe, and infrared emission accompanying rare gas and impurity quenching.

Julian Few and Gus Hancock

Department of Chemistry, University of Oxford, Physical and Theoretical Chemistry Laboratory,
South Parks Road, Oxford OX1 3QZ

Abstract

The quenching rates of $\text{NO}(A^2\Sigma^+, v=0)$ with He, Ne, Ar, Kr and Xe have been studied at room temperature by measurements of the time dependence of the fluorescence decay following laser excitation. The rates are slow, with upper limits of rate constants determined as between 1.2 and $2.0 \times 10^{-14} \text{ cm}^3 \text{ molecule}^{-1} \text{ s}^{-1}$, considerably lower than those reported before in the literature. Such slow rates can be markedly influenced by impurities such as O_2 and H_2O which have quenching rate constants close to gas kinetic values. Time resolved Fourier transform infrared emission has been used to observe the products of the quenching processes with the rare gases and with impurities. For He, Ne Ar and Kr there is no difference within experimental error of the populations in $\text{NO}(X^2\Pi, v \geq 2)$ produced with and without rare gas present, but the low quantum yields of such quenching (of the order of 5% for an atmosphere of rare gas) preclude quantitative information on the quantum states being obtained. For quenching by Xe the collisional formation of electronically excited Xe atoms dominates the emission at early times. Vibrationally excited $\text{NO}(X^2\Pi, v)$ and products of reactive quenching are observed in the presence of O_2 and H_2O .

Introduction

The quenching rate constants of $\text{NO}(\text{A}^2\Sigma^+, v=0)$ by the rare gases at room temperature are generally considered to be small in comparison with gas kinetic collision values. For quenching by Ar, the most widely studied rare gas, rate constants have been reported as $8.1 \pm 1.9 \times 10^{-13}$,¹ $3.9 \pm 0.2 \times 10^{-13}$,² $< 2 \times 10^{-13}$,³ *ca.* 1×10^{-13} ,⁴ $6.9 \pm 2.7 \times 10^{-14}$,⁵ $< 4.2 \times 10^{-14}$,⁶ and 3.6×10^{-14} ⁷ $\text{cm}^3 \text{ molecule}^{-1} \text{ s}^{-1}$ at room temperature, a span of over an order of magnitude. Often such rate constants have been described as upper limits because of the potential interference from low concentrations of impurities such as O_2 and H_2O , which have far higher values of *ca.* 1.5×10^{-10} ,^{2,3,5-9,10-16} and 8×10^{-10} ,^{2,3,6,7,9,13-15} $\text{cm}^3 \text{ molecule}^{-1} \text{ s}^{-1}$ respectively, and the susceptibility of the measured rare gas quenching rate constants to impurity levels has been noted.^{1,2,7}

In a recent set of studies we have observed the products of the collisional quenching of $\text{NO}(\text{A}^2\Sigma^+, v=0)$ using the technique of Time Resolved Fourier Transform InfraRed Emission (TRFTIRE).^{17,18} The method has enabled the distribution of ground state vibrationally excited $\text{NO}(\text{X}^2\Pi)$ products to be measured, as well as the observation of vibrationally excited quenching molecules and reaction products. In these experiments, it is desirable to maximise the quenching quantum yield of the added collider, so that processes of fluorescence and self quenching (by NO) can be easily discriminated. In our previous studies of quenching by NO,¹⁷ CO_2 ,¹⁸ and N_2O ¹⁸ modest pressures (0.5 – 5 Torr) were required to achieve a quantum yield for collisional quenching of >50%, because the quenching rate constants with these collision partners are close to gas kinetic. If we wish to observe quenching by the rare gases, high pressures would be needed to ensure an adequate quenching quantum yield. For example, for the slowest rate constant reported for quenching by Ar,⁷ an atmosphere of the gas would result in a quenching quantum yield of only 0.15.

Measurements on the other rare gases are sparse. Greenblatt and Ravishankara determined the rate constant for quenching by Ne as $< 1.2 \times 10^{-13} \text{ cm}^3 \text{ molecule}^{-1} \text{ s}^{-1}$,⁶ and Nee *et al.*⁵ reported rate constants for He and Xe as $2.0 \pm 0.4 \times 10^{-13}$ and $1.38 \pm 0.21 \times 10^{-12} \text{ cm}^3 \text{ molecule}^{-1} \text{ s}^{-1}$ respectively. The value for Xe is the highest reported for any rare gas. It implies that 760 Torr of Xe would, under our TRFTIRE conditions, reduce the fluorescence lifetime from the radiative value of *ca.* 200 ns^{15,16,19} to some 25 ns, resulting in a quenching quantum yield of *ca.* 90%, and thus would allow the observation of the products of a dominant quenching process where only inelastic transfer would be observed. We have carried out preliminary studies of the infrared emission which accompanies quenching by Xe, and in the course of these investigations we have additionally observed the uv fluorescence from the $\text{NO}(\text{A}^2\Sigma^+, v=0)$ state in order to normalise the infrared signal for any variations of uv pumping laser intensity.¹⁷ We find that close to an atmosphere of Xe changes the fluorescence lifetime by less than 10%, and thus the reported rate constant⁵ appears to be an overestimate of the true value. This prompted an investigation into the quenching rate constants for all the rare gases which is reported here. In addition, TRFTIRE experiments were carried out with the rare gases as quenchers, together with measurements on O_2 and H_2O as potential contaminants.

Experimental

a) Fluorescence decay rates.

The reaction cell was of stainless steel, internal volume 1500 cm³ fitted with quartz windows and pumped with a turbomechanical pump (Leybold TurboVac 51C). Pressures were measured with a Penning gauge (10⁻⁷ - 10⁻³ Torr) and capacitance manometers (full scale ranges 10 and 1000 Torr). NO at pressures of the order of 2-5 mTorr was optically pumped at 226.25 nm, a band head of the overlapped Q₁₁ and P₂₁ lines of the A(²Σ⁺, v=0) – X(²Π_{1/2}, v=0) transition. The radiation was generated by a tunable dye laser (SIRAH Cobra Stretch SFM 355) pumped by a Nd-YAG laser (Continuum Powerlite Precision II 8010), with 226 nm radiation of bandwidth 0.1 cm⁻¹ (0.46 pm) formed by frequency mixing the single mode YAG third harmonic with tunable dye laser radiation of bandwidth 3.5 pm near 624 nm. The laser output energy was attenuated from the normal levels to ca. 50 μJ/pulse in order to reduce saturation effects. Red shifted laser induced fluorescence (LIF) was observed at right angles to the propagating laser beam at wavelengths between 345 and 400 nm through a series of optical filters by means of a photomultiplier tube (Thorn EMI 9813QB). The observed wavelengths are for transitions between A(²Σ⁺, v=0) → X(²Π, v=9-11), which have low Franck Condon factors but allow good discrimination between fluorescence and scattered laser light. Signals were digitised and averaged for some 1000 laser shots (LeCroy 44MXs-A) and the decays analysed as a single exponential with commercial software.

The rare gases (BOC) had the following stated purities: He >99.995%, Ne >99.994%, Ar >99.9995%, Kr >99.999%, Xe >99.999%. All gases were admitted to the reaction vessel through stainless steel tubes, and the rare gases were passed through absorption tubes to remove traces of the fast quenchers H₂O (All-Pure) and O₂ (OxiClear) to specified levels of < 1 and < 5 ppb respectively. NO (MG Gases, 99.5%) was purified as before to remove any NO₂:¹⁸ CO₂ (BOC >99.995%) was used without further purification.

The reaction cell was evacuated to a base pressure of 1 x 10⁻⁶ Torr, and had a measured external leak rate (Leybold Phoenix leak detector) of less than 1 x 10⁻⁸ Torr s⁻¹. When the cell was closed to the pump the pressure rose at a rate of 2.5 x 10⁻⁶ Torr s⁻¹, presumably through surface desorption. All experiments were carried out at room temperature, 295 K.

b) Infrared emission

TRFTIRE experiments were carried out with the rare gases, O₂ and H₂O as quenchers of NO(A²Σ⁺, v=0). The details of the procedures used have been described in detail,^{17,18} and only an outline is given here. NO at a pressure of 50 mTorr was pumped by the same laser system as described above, but now at a higher laser energy (ca. 2 mJ/pulse) in order to maximise the signal. IR emission was observed as a function of time following irradiation (typically 2 μs resolution in these experiments) by an FTIR spectrometer (Bruker IFS/66) operating in step-scan mode. Spectra recorded with an InSb detector (Grasbey IS2) are presented in the NO X²Π Δv=-2 overtone region between 2500 and 4000 cm⁻¹, with the resolution normally set at 20 cm⁻¹. O₂ (BOC >99.5%) was used without further purification: demineralised H₂O was purified by freeze-thaw cycling before being admitted as vapour to the reaction vessel.

Results

a) Quenching rates of NO ($A^2\Sigma^+$, $v=0$)

Measurements were first carried out with CO_2 as a quencher in order to compare results with the many previous determinations of the rate constant at room temperature. Figure 1 shows the fluorescence decay rate of a sample of ca. 2 mTorr NO as a function of CO_2 concentration, with the slope yielding a rate constant of $(4.16 \pm 0.04) \times 10^{-10} \text{ cm}^3 \text{ molecule}^{-1} \text{ s}^{-1}$ and with an intercept of $(5.09 \pm 0.04) \times 10^6 \text{ s}^{-1}$. All quoted statistical errors are at the 1σ level, and are discussed in detail below for the measurements on the rare gases.

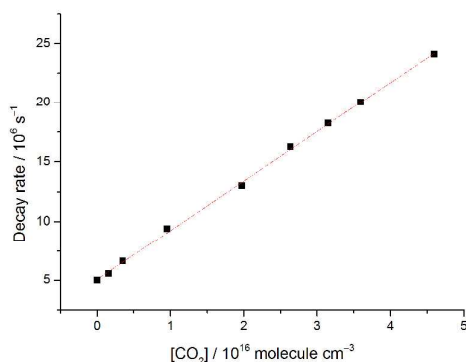


Figure 1. Decay rates of the fluorescence from $\text{NO}(A^2\Sigma^+, v=0)$ as a function of CO_2 concentration. The best fit straight line shown yields a quenching rate constant of $(4.16 \pm 0.04) \times 10^{-10} \text{ cm}^3 \text{ molecule}^{-1} \text{ s}^{-1}$.

Previous measurements of the rate constant have ranged from $3.6 - 5.0 \times 10^{-10} \text{ cm}^3 \text{ molecule}^{-1} \text{ s}^{-1}$ ^{2-7,10,15} with the most recent determination (which has the lowest reported statistical error bars) of $(4.09 \pm 0.02) \times 10^{-10} \text{ cm}^3 \text{ molecule}^{-1} \text{ s}^{-1}$ ¹⁵ in excellent agreement with the present data. The intercept should equal the sum of the rates of radiative decay and quenching by the parent NO molecule. The radiative decay rate is reported as between 4.90 and $5.21 \times 10^6 \text{ s}^{-1}$,^{16,19}. The rate constant for self quenching is fast,^{5,14-16} but the low pressure of ca. 2 mTorr NO means that its contribution to the overall decay rate is negligible (an additional $2 \times 10^4 \text{ s}^{-1}$). The intercept of Figure 1 at zero CO_2 concentration is within the expected range, and our results thus give confidence to the measurements of decay rates in this experiment.

Figure 2 shows the effect on the LIF traces of the addition of rare gas, in this case Kr.

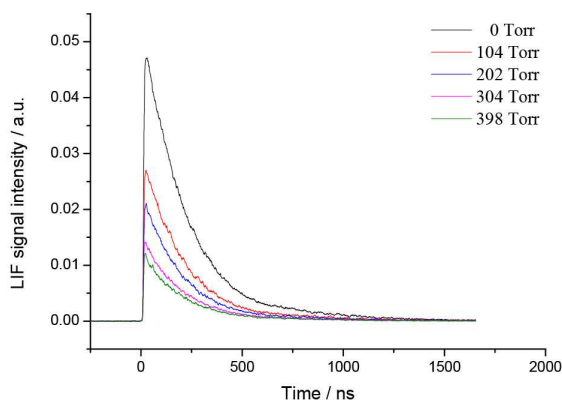


Figure 2. LIF kinetic decays following the excitation of $\text{NO}(A^2\Sigma^+, v=0)$ as a function of pressure of Kr, showing the marked reduction in intensity of the fluorescence with increasing Kr pressure.

The first clear effect is the reduction of the magnitude of the LIF signal with increasing pressure until a limiting value is reached at the highest pressures used, which were close to atmospheric for all the rare gases. The reduction was larger for the heavier rare gases, and is attributed to pressure broadening of the pumped transitions. For example, for Ar the measured pressure broadening coefficient of $0.5 \text{ cm}^{-1} \text{ atm}^{-1}$ ^{20,21} would result in the absorption of an isolated feature at line centre at a pressure of 300 Torr to decrease to some 40% of its value when collisional broadening is negligible, and this value is equal within experimental error to the observed reduction in the intensity of the fluorescence. Such broadening makes a marginal decrease in the signal to noise ratios of the present measurements, but does not affect the kinetics: the effect however will be discussed below when previous Stern-Volmer analyses are considered. The second effect is that the decay rates change only slightly by the addition of up to 600 Torr Kr. This set of data are plotted as a function of Kr concentration in Figure 3, and show a measured increase in rate of only 7% over the sum of the radiative and self quenching decay rates at the highest pressure used.

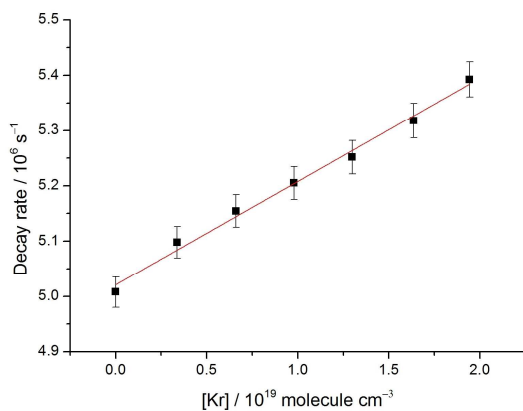


Figure 3. Decay rates of the fluorescence from $\text{NO}(A^2\Sigma^+, v=0)$ as a function of Kr concentration. The error bars shown are for an uncertainty (FWHM) of 2.2 ns in the measured decay rate as explained in the text. The straight line fitted to this data set yields a quenching rate constant of $(1.9 \pm 0.1) \times 10^{-14} \text{ cm}^3 \text{ molecule}^{-1} \text{ s}^{-1}$, and the average of five such plots is shown as the rate constant in Table 1.

The rate constants obtained from the slopes of plots such as in Figure 3 will result in considerable errors because of the narrow range of decay rates measured, and we now consider these. First, the decay rates, averaged over 1000 laser shots, were found to have low statistical errors (*ca.* 0.2 ns), and of the order of the time resolution of the A-D convertor (0.25 ns). Digitisation error caused by the 8 bit A-D convertor will only be significant at long time delays, and separate fits over 3, 4 and 5 fluorescence lifetimes showed consistent values with no clear deviations from a single exponential decay. The capacitance manometer (previously calibrated against a Hg column) introduces an error smaller than the dimension of the symbols in Figure 3. It can be seen however that the points in Figure 3 appear to show random deviations from a straight line which are larger than these error limits. Although the pressure of NO in the cell (normally 5 mTorr) could only be measured to the nearest 1 mTorr, such a variation would produce a systematic drift of the decay rate of the order of 10^4 s^{-1} and appears not to be the cause. A potential significant error arises from the jitter in the arrival time at the anode of the photomultiplier of current pulses caused by single photoelectrons emitted from the cathode, quoted by the manufacturer as 2.2 ns (FWHM), and error bars of this magnitude (approximately 1% of the measured decay times) are shown in Figure 3. They appear to encompass the data, and are the largest errors that we can quantify with any precision. The best fit straight line for the plot in Figure 3, with the points weighted for their error bars gives a slope of $(1.9 \pm 0.1) \times 10^{-14} \text{ cm}^3 \text{ molecule}^{-1} \text{ s}^{-1}$. We note that error bars of this magnitude are smaller than the size of the symbols in Figure 1, where the decay rates span a far larger range.

For each rare gas, five or six separate runs were carried out to produce plots such as shown in Figure 3, and the slopes averaged to produce values of rate constants. Table 1 shows the results, all in the region of $(1-2) \times 10^{-14} \text{ cm}^3 \text{ molecule}^{-1} \text{ s}^{-1}$, together with previous reports. It can be seen that the present rate constants are without exception the lowest values reported, and agree only with previous measurements when the latter are given explicitly as upper limits.

We now consider what are probably the largest source of error in these experiments, the effect of impurities. The rate constants reported in Table 1 show that an atmosphere of added gas yields quenching rates of $(3-5) \times 10^5 \text{ s}^{-1}$. Impurities with the largest effect will be O_2 and H_2O (quenching by N_2 is negligible at room temperature,^{2,6,7,11,13,15,16,22,23}) and if the average of the quenching rates shown in Table 1 was solely caused by impurities, it would correspond to partial pressures of $\text{O}_2 = 80$ mTorr and $\text{H}_2\text{O} = 15$ mTorr (105 and 20 ppm respectively at 1 atmosphere). Stated upper limits for impurities of the rare gases are between 5 ppm (Ar) and 60 ppm (Ne), and thus prepurification was necessary, particularly for Ne: indeed measurements carried out without the H_2O and O_2 filters yielded rates which were considerably higher for He and Ne. The absorbing filters, if working to specification, would reduce the levels of O_2 and H_2O to a few μTorr , yielding a negligible impurity quenching effect. External leak rates over the duration of a single experiment (*ca.* 20 minutes) would similarly yield negligible quenching. Desorption from the vessel walls however would imply a partial pressure of 3 mTorr impurity over this time scale, and as the experiments were carried out with increasing amounts of rare gas added as a function of time the largest pressure of impurity would accompany the largest pressure of rare gas. If the desorbed gas was 100% H_2O (the fastest

quencher) it would account for a quenching rate of $8 \times 10^4 \text{ s}^{-1}$ for the final (highest pressure) measurement point, and $1.5 \times 10^4 \text{ s}^{-1}$ if the desorbed gas was purely oxygen. These are not negligible values, and thus from this section we would consider our results of Table 1 as upper limits for the true rate constants. The error limits given in Table 1 are those from an averaging of the individual runs, and it can be seen for example for the Kr data that the spread of values is larger than that for the individual run shown in Figure 3. A potential explanation is that variations of impurity levels (particularly water vapour) have occurred in the different runs with a given rare gas. Quoting the results of Table 1 as upper limits is consistent with this possibility.

b) Products of the quenching of NO A($^2\Sigma^+$, $v=0$).

In an attempt to assess the importance of impurity quenching, we have used the TRFTIRE method to observe the products of the quenching process with rare gases and with potential impurities O_2 and H_2O . Figure 4 shows examples of the emission spectra at $5 \mu\text{s}$ following the irradiation of 50 mTorr NO with 50 and 400 Torr of purified Ar.

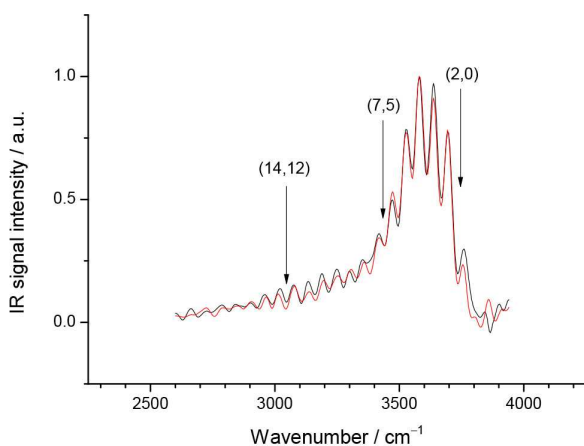


Figure 4. Infrared emission observed at $5 \mu\text{s}$ following irradiation of 50 mTorr NO to form NO A($^2\Sigma^+$, $v=0$) in the presence of 50 (black trace) and 400 (red trace) Torr Ar. Band origins of the first overtone transitions in NO($X^2\Pi$) are shown.

Quantum yields for the three processes of fluorescence, quenching by NO and quenching by the rare gas (given as upper limits from the data of Table 1) are 92%, 7.8%, $\leq 0.3\%$ (50 Torr Ar) and 89.5%, 7.5%, $\leq 3\%$ (400 Torr Ar). Emission is identified as first overtone transitions in the ground state of NO ($X^2\Pi \Delta v=-2$), with the expected clear minima seen at the band origins.¹⁷ The emission spectra at early times are indistinguishable within experimental error from those observed in the absence of high pressures of the rare gas: fluorescence dominates the formation of low vibrational levels of NO ($X^2\Pi v \leq 6$), and self quenching is responsible for the higher levels.¹⁷ The spectra with Ar should not be severely affected by vibrational de-excitation over the time scale of Figure 4. For Ar the fastest measured rate for vibrational relaxation, for $v = 12$, is $(24 \pm 14) \times 10^{-16} \text{ cm}^3 \text{ molecule}^{-1} \text{ s}^{-1}$ ²⁴ implying a loss of 14% at $5 \mu\text{s}$. The results suggest that emission from any vibrationally excited NO($X^2\Pi$) formed by Ar quenching is swamped by that formed by fluorescence and self quenching. Little can be learnt about the quantum states in NO($X^2\Pi$) produced, except that Ar does not appear to give a marked

increase in the population of the higher vibrational levels which are produced by NO self quenching with a similar quantum yield. The same conclusion can be made from the spectra observed in the quenching by He, Ne and Kr (Xe is discussed below).

Figure 5 shows the early time (4 μ s) TRFTIRE spectrum in the presence of 400 Torr Ar and 1.17 Torr O₂. Here the quantum yields of fluorescence and collisional quenching by O₂ are both approximately 50%, and the additional production of high vibrational levels of NO X² Π is evident from a comparison of this Figure with the data presented in Figure 4.

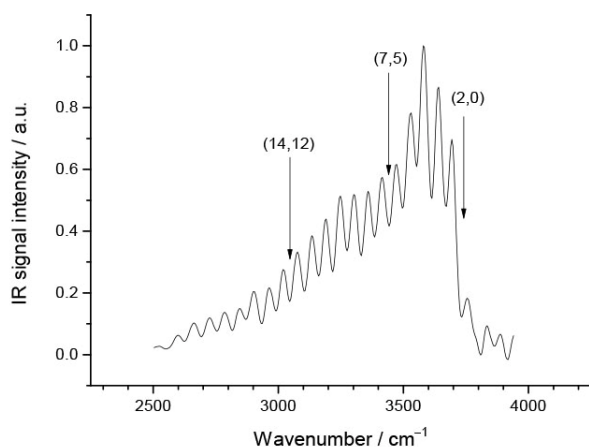


Figure 5. Infrared emission observed at 4 μ s following the irradiation of 50 mTorr NO, 400 Torr Ar and 1.17 Torr O₂. Band origins of the first overtone transitions in NO(X² Π) are shown.

If the observed increase in quenching rate in the presence of 400 Torr Ar (3%) was solely caused by O₂ it would correspond to an impurity level of 32 mTorr (80 ppm). From results such as that shown in Figure 5 we have determined the nascent populations of NO (X² Π , ν) formed by O₂ quenching,²⁵ and find that they result in a lower degree of vibrational excitation than that measured for self quenching.¹⁷ From these data we calculate that an impurity level of 80 ppm O₂ would give rise to an increase in the high vibrational level populations which would be unobservable within experimental error: for example the populations between $\nu = 8$ and $\nu = 14$ would increase by 15% compared with those formed (by self quenching) in the absence of Ar, and given that these levels would be affected to approximately this degree by Ar vibrational quenching we cannot redefine our measurement of the quenching decay rate in Table 1 as being other than an upper limit. We note that quenching by O₂ also produces vibrationally excited NO₂ as a reaction product, and an upper limit of 18% is derived for its quantum yield.²⁵ In the absence of Ar this gives rise to strong emission in the $\Delta\nu_1 = \Delta\nu_3 = -1$ band near 2700 cm⁻¹, overlapping the overtone emission from high vibrational levels of NO(X² Π , ν). 400 Torr Ar removes the NO₂ emission rapidly by efficient vibrational quenching of the triatomic, and hence is unobserved in the data of Figure 5.

We next turn to quenching by H₂O. Figure 6 shows the TRFTIRE spectra for irradiation of 50 mTorr NO in the presence of 200 mTorr H₂O and 50 Torr Ar at 5 μ s following irradiation. Here the quantum yields for quenching by fluorescence and by H₂O are both approximately 50%: Ar is present to increase the fraction of NO excited to the A² Σ^+ state through rotational hole filling.¹⁷

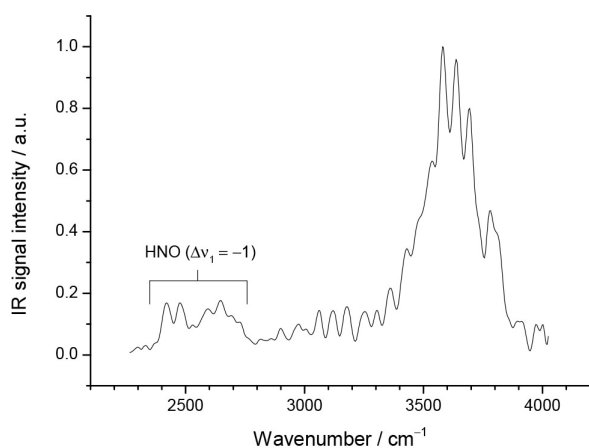


Figure 6. Infrared emission observed at 3 μs following the irradiation of 50 mTorr NO, 50 Torr Ar and 200 mTorr H₂O. Marked are the positions of the $\Delta v_1 = -1$ bands of HNO, and some structure corresponding to the first overtone transitions of NO($X^2\Pi$) can be seen underlying the strong emission near 3600 cm^{-1} believed to be from O-H stretching transitions.

We observe an intense emission near 3600 cm^{-1} at early times, which is rapidly quenched to reveal the underlying longer lived and structured first overtone emission from NO, which is about a factor of 3 less intense. We assign the carrier of this emission to the O-H stretch of either H₂O formed by energy transfer, or to potentially reactive quenching products such as OH or HONO, and we note that H atoms have been reported as resulting from the reactive quenching process which presumably also produces HONO.²⁶ Emission near 2600 cm^{-1} is identified as the $\Delta v_1 = -1$ band of HNO, consistent with a reactive channel which also forms OH. Again we use this information simply to estimate whether or not the observed emission in the presence of Ar could be the result of impurity. The 3% additional quenching rate measured with 400 Torr Ar would correspond to a pressure of 6 mTorr H₂O impurity. A comparison of the early and late time emission near 3600 cm^{-1} would indicate that 6 mTorr H₂O would increase the signal by some 15% compared with that with zero H₂O. Again this comparative amount is within our experimental error of determining such signal ratios.

The TRFTIRE data for the rare gases He, Ne, Ar and Kr lead to the conclusion that the infrared emission observed in the presence of the rare gases cannot provide us with additional information on the accuracy of the rate constants in Table 1. The one example where we do see a remarkably different emission spectrum from that resulting from fluorescence and self quenching is in the presence of Xe, where the signal over the wavenumber region of the NO first overtone is dominated at early times by atomic emission from electronically excited Xe atoms, and identified as Xe $5p^55d \rightarrow 5p^56p$ transitions between 2750 and 3800 cm^{-1} .²⁷ There are isolated two photon transitions in Xe at 225.51 and 226.34 nm which we observe to give rise to atomic IR emission following excitation of Xe alone. However, when NO is added the Xe atomic emission is additionally observed at all excitation wavelengths corresponding to features within the NO($A^2\Sigma^+ - X^2\Pi$) absorption spectrum. The emission is found to have a squared dependence on laser power, and has a slower rise time than that produced following excitation at the isolated two photon transitions in Xe. It appears consistent with two photon excitation of NO to states which undergo collisional energy exchange with Xe. Two photon excitation of NO has been shown to be a process of low probability in our TRFTIRE experiments,¹⁷ and the relatively high atomic emission intensity is a result of the Einstein A factors

for these transitions being 4 - 5 orders of magnitude larger²⁸ than those for the NO ($X^2\Pi v \rightarrow v-2$) overtones.²⁹

Discussion.

Table 1 shows that our rate constants for quenching by the five rare gases are all slower than those reported as explicit values in the literature, and, as has been previously noted,^{1,2,7} this evidence points to the importance of impurity quenching in such studies. We cannot eliminate such quenching from our experiments by looking at the effect that impurities would have on the infrared emission, as the sensitivity of the TRFTIRE observations is insufficient to distinguish these low quenching quantum yield processes from those of fluorescence and self quenching. We cannot estimate with certainty the concentration of impurities in our system, one reason being that we cannot be certain of the efficacy of the H₂O and O₂ filters. If the impurity levels are caused purely by degassing of the chamber walls (ie the purification processes for the rare gases were working to specification) and if we assume that desorption produces H₂O, the fastest quencher, so that its partial pressure is 3 mTorr for the highest pressure of quenching gas used, this would contribute $8 \times 10^4 \text{ s}^{-1}$ to the decay rate. If this is the sole impurity effect then lower limits to the rate constants would become between 65 and 80% of the values quoted in Table 1. However, because of the abovementioned uncertainties in the purification procedure for the rare gases, and because of the uncertainty in the nature of any degassing process, we choose to present our measurements as upper limits to the true rate constant values.

The higher values of previously reported rate constants shown in Table 1 can largely be attributed to impurity effects, but there is one notable exception, and that is the rate constant reported by Nee *et al.* for quenching by Xe, almost a factor of 100 larger than the present result.⁵ Impurities cannot account for the discrepancy, given that vuv absorption was used by Nee *et al.* to check impurity levels, and this would have presumably shown the presence of O₂ and H₂O. In this work however a Stern-Volmer analysis of fluorescence was employed rather than the fluorescence decay measurements used for the majority of the studies of Table 1, and this method relies upon the rate of production of the upper fluorescing state by photon absorption being invariant with rare gas concentration. Figure 2 shows that in the present experiments this is not the case, and can be accounted for by pressure broadening: for example, the addition of 300 Torr Xe in our experiments reduced the intensity of the fluorescence by a factor of 3, and a Stern-Volmer treatment of such a reduction would yield a rate constant of $1.2 \times 10^{-12} \text{ cm}^3 \text{ molecule}^{-1} \text{ s}^{-1}$, almost a factor of 100 larger than our directly measured value. In the present experiments the dye laser output bandwidth (0.1 cm^{-1}) is always smaller than that of the absorption feature excited, and the pressure broadening effect will be clear: however if the bandwidth of the excitation source is always larger than the absorption feature then such an effect will disappear, and a Stern-Volmer analysis will be valid. This should be the case in the experiments of Nee *et al.*, as they measured the fluorescence intensity integrated over the whole of the absorption spectrum.⁵ We thus cannot use this argument to explain the discrepancies between the two sets of Xe measurements. We note that Settersten *et al.*¹⁵ have remarked that the rate constant measured by Nee *et al.* using the Stern Volmer method for quenching by nitrogen, another gas where high pressures were needed, is again higher than the

currently accepted value, and a similar trend can also be seen in their observations on He and Ar quenching as shown in Table 1.

Table 1 shows that within experimental error the cross sections for the collisional energy transfer processes show a mild increase with increased mass of rare gas. Such an increase would be expected from one of the several models which have been applied to $\text{NO}(A^2\Sigma)$ quenching, namely the collision complex model, where the formation of an electronically excited adduct is the rate controlling step, and its relative concentration (and hence the cross section for energy transfer) is controlled by long range attractive forces.^{30,31} Such a model however has failed to account for the behaviour of low cross section quenchers such as CO and N_2 , and an alternative model based on energy transfer to nearby $a^4\Pi$, $b^4\Sigma$ or $B^2\Pi$ states has been suggested.⁷ Such processes will have activation barriers (the curve crossings between $\text{NO}(A^2\Sigma)$ and these states lie some $2500 - 7000 \text{ cm}^{-1}$ above the energy of $v=0$) and the rates would be expected to increase markedly with temperature. Temperature dependent measurements have been carried out for Ar, but show little effect.^{1,7} Other models applied to NO quenching include the harpoon mechanism and its variants,^{10,11,32} but again are inapplicable to the rare gases.⁷ What are required for a quantitative description of the cross sections are scattering calculations on the potential energy surfaces for the NO-rare gas triatomic systems for NO in its $X^2\Pi$ and $A^2\Sigma$ states. Such surfaces have been recently constructed³³⁻³⁵ and used for the determination of the absorption spectroscopy of the van der Waals NO-rare gas systems in the A-X transitions,³³ and for scattering calculations of both differential cross sections for rotationally inelastic transfer³⁶ and collisional depolarisation rate constants for the upper $\text{NO}(A^2\Sigma)$ state.^{37,38} Trajectory surface hopping calculations such as those successfully carried out for quenching of the A state of OH to the ground X state in collisions with Kr³⁹ could conceivably be carried out on these surfaces to yield the quenching cross section in the electronically equivalent NO A-X transition. However, it should be pointed out that the measured cross section for quenching of OH by Kr, $5-10 \times 10^{-16} \text{ cm}^2$ depending upon rotational level,³⁹⁻⁴² is over three orders of magnitude larger than that for NO reported in Table 1. This must reflect the very different degrees of overlap of the two sets of surfaces, and suggests that the trajectory calculations of the cross sections for NO quenching could be a stringent test of the precision of the calculated surface intersection points.

Conclusions

Measurements of rate constants at room temperature for the collisional quenching of $\text{NO}(A^2\Sigma^+, v=0)$ with He, Ne, Ar, Kr and Xe have produced values which are consistently lower than the explicit values previously reported. Impurity effects appear to be responsible for the many previous overestimations of the rate constants made from observations of the time resolved fluorescence from the $\text{NO}(A^2\Sigma^+, v=0)$ state. Discrepancies arise between the present results and far higher values reported from Stern-Volmer analyses of the fluorescence quenching, but the explanation for this is unclear. Time resolved Fourier transform infrared emission observations in the presence of the rare gases showed no additional emission attributable to the production of vibrationally excited $\text{NO}(X^2\Pi, v)$, but because of the low rare gas quenching quantum yields achieved in these experiments, the only conclusion possible is that the quenching does not result in the production of highly vibrationally excited levels of $\text{NO}(X^2\Pi)$. Infrared emission resulting from quenching by

potential impurities O_2 and H_2O is reported, but these observations were unable to provide lower limits for the rate constants. The rate constants are thus reported as upper limits.

Acknowledgements

This work was supported by the EPSRC programme grant EP/G00224X/1: New Horizons in Chemical and Photochemical Dynamics. JF is grateful to the EPSRC for the award of a studentship. We thank Sara Gowrie and Greg Dunning for help with early versions of these experiments.

Rare Gas	Rate constant/ 10^{-14} $\text{cm}^3 \text{ molecule}^{-1} \text{ s}^{-1}$	Reference	Cross section/ 10^{-19} cm^2
He	$\leq 2.0 \pm 0.5$ 20 ± 4	This work 5	$\leq 1.6 \pm 0.4$
Ne	$\leq 1.7 \pm 0.4$ < 12	This work 6	$\leq 2.3 \pm 0.5$
Ar	$\leq 1.2 \pm 0.4$ 81 ± 19 39 ± 2 < 20 <i>ca.</i> 10 6.9 ± 2.7 < 4.2 3.6	This work 1 2 3 4 5 6 7	$\leq 2.0 \pm 0.7$
Kr	$\leq 1.8 \pm 0.2$	This work	$\leq 3.4 \pm 0.4$
Xe	$\leq 1.6 \pm 0.2$ 138 ± 21	This work 5	$\leq 3.2 \pm 0.4$

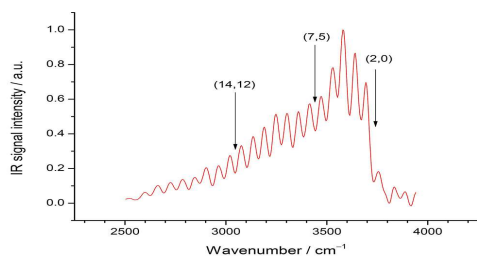
Table 1. Values of the measured rate constants for quenching of $\text{NO}(A^2\Sigma^+, v=0)$ by He, Ne, Ar, Kr, and Xe at room temperature, together with previous values reported in the literature. Present values are given as upper limits because of the potential effect of impurities as discussed in the text.

References

1. J.A. Gray, P.H. Paul and J.L. Durant, *Chem. Phys. Lett.*, 1992, **190**, 266.
2. I.S. McDermid and J.B. Laudenslager, *J. Quant. Spectry. Radiative Transfer*, 1982, **27**, 483.
3. P.H. Paul, J.A. Gray, J.L. Durant Jr. and J.W. Thoman Jr., *Chem. Phys. Lett.*, 1996, **259**, 508.
4. A.B. Callear and I.W.M. Smith, *Trans. Far. Soc.*, 1963, **59**, 1720.
5. J. B. Nee, C. Y. Juan, J. Y. Hsu, J. C. Yang and W. J. Chen, *Chem. Phys.*, 2004, **300**, 85.
6. G.D. Greenblatt and A.R. Ravishankara, *Chem. Phys. Lett.*, 1987, **136**, 501.
7. M. C. Drake and J. W. Ratcliffe, *J. Chem. Phys.*, 1993, **98**, 3850.
8. L.A. Melton and W. Klemperer, *Planet. Space Sci.*, 1972, **20**, 157.
9. I. M. Campbell and R.S. Mason, *J. Photochem.*, 1978, **8**, 321.
10. M. Asscher and Y. Haas, *J. Chem. Phys.*, 1982, **76**, 2115.
11. Y. Haas and G.D. Greenblatt, *J. Phys. Chem.*, 1986, **90**, 513.
12. L.R. Mauldin and A.R. Ravishankara, *J. Phys. Chem.*, 1986, **90**, 4923.
13. G. A. Raiche and D. R. Crosley, *J. Chem. Phys.*, 1990, **92**, 5211.
14. R. Zhang and D.R. Crosley, *J. Chem. Phys.*, 1995, **102**, 7418.
15. T.B. Settersten, B.D. Patterson and J.A. Gray, *J. Chem. Phys.*, 2006, **124**, 234308.
16. T. B. Settersten, B. D. Patterson and C. D. Carter, *J. Chem. Phys.*, 2009, **130**, 204302.
17. G. Hancock and M. Saunders, *Phys. Chem. Chem. Phys.*, 2008, **10**, 2014.
18. M.A.B. Paci, J. Few, S. Gowrie and G. Hancock, *Phys. Chem. Chem. Phys.*, 2013, **15**, 2554.
19. J. Luque and D.R. Crosley, *J. Chem. Phys.*, 2000, **112**, 9411.
20. A. Y. Chang, M. D. DiRosa and R. K. Hanson, *J. Quant. Spectry. Radiative Transfer*, 1992, **47**, 375.
21. A. O. Vydrov, J. Heinze and U. E. Meier, *J. Quant. Spectry. Radiative Transfer*, 1995, **53**, 277.
22. T. Imago, K. Shibuya, K. Obi and I. Tanaka, *J. Phys. Chem.*, 1986, **90**, 6006.
23. J.W. Thoman, J.A. Gray, J.L. Durant and P.H. Paul, *J. Chem. Phys.*, 1992, **97**, 8156.
24. G. Hancock, M. Morrison and M. Saunders, *Phys. Chem. Chem. Phys.*, 2009, **11**, 8507.
25. J. Few, D.Phil thesis Oxford University (2013).
26. H. Umemoto, N. Terada, K. Tanaka, T. Takayanagi, Y. Kurosaki and K. Yokoyama, *Chem. Phys.*, 2000, **259**, 39.
27. NIST Atomic Spectra Database <http://www.nist.gov/pml/data/asd.cfm>
28. A. Dasgupta, J. P. Apruzese, O. Zatsarinny, K. Bartschat and C. Froese Fischer, *Phys. Rev. A*, 2006, **74**, 012509.
29. S. R. Langhoff, C. W. Bauschlicher Jr. and H. Partridge, *Chem. Phys. Lett.*, 1994, **223**, 416.
30. C. S. Parmenter and M. Seaver, *J. Chem. Phys.*, 1979, **70**, 5458.
31. H.-M. Lin, M. Seaver, K. Y. Tang, A. E. W. Knight and C. S. Parmenter, *J. Chem. Phys.*, 1979, **70**, 5442.
32. P. H. Paul, J. A. Gray, J. L. Durant, Jr. and J. W. Thoman, Jr., *Appl. Phys. B*, 1993, **57**, 249.
33. J. Kłos, M.H. Alexander, R. Hernández-Lamonedá and T.G. Wright, *J. Chem. Phys.*, 2008, **129**, 244303.
34. O.V. Ershova and N.A. Besley, *J. Chem. Phys.*, 2012, **136**, 244313.
35. H. Cybulski and B. Fernandez, *J. Phys. Chem. A*, 2012, **116**, 7319.
36. J. J. Kay, J. D. Steill, J. Kłos, G. Paterson, M. L. Costen, K. E. Strecker, K. G. McKendrick, M. Alexander and D. W. Chandler, *Mol. Phys.*, 2012, **110**, 1693.

37. M. Brouard, H. Chadwick, Y.-P. Chang, C. J. Eyles, F. J. Aoiz and J. Kłos, *J. Chem. Phys.*, 2011, **35**, 084306.
38. G. Paterson, M.L. Costen and K.G. McKendrick, *Int. Rev. Phys. Chem.*, 2012, **31**, 69.
39. J.H. Lehman, M.I. Lester, J. Kłos, M.H. Alexander, P. J. Dagdigan, D. Herráez-Aguilar, F. J. Aoiz, M. Brouard, H. Chadwick, T. Perkins and S.A. Seamons, *J. Phys. Chem. A*, 2013, **117**, 13481.
40. I. J. Wysong, J. B. Jeffries, and D. R. Crosley, *J. Chem. Phys.*, 1990, **92**, 5218.
41. D. E. Heard and D. A. Henderson, *Phys. Chem. Chem. Phys.*, 2001, **2**, 67.
42. B.L. Hemming, D.R. Crosley, J.E. Harrington and V. Sick, *J. Chem. Phys.*, 2001, **115**, 3099.

Contents page:



Rates of quenching of NO ($A^2\Sigma^+ v=0$) have been measured for the rare gases, and infrared emission used to observe vibrationally excited quenching products. The figure shows emission following quenching by O₂, a potential contaminant.